Naval Research Laboratory

Washington, DC 20375-5320

NRL/MR/6110--14-9506

Aerolization During Boron Nanoparticle Multi-Component Fuel Group Burning Studies

Joseph P. Smith
Michael T. Montgomery

Chemical Dynamics and Diagnostics Branch
Chemistry Division

Stephen M. Masutani
Brandon A. Yoza
Ryan Kurasaki
Christopher Kinoshita

University of Hawaii
Honolulu, Hawaii

Richard B. Coffin

Chemical Dynamics and Diagnostics Branch
Chemistry Division

February 3, 2014

REPORT DOCUMENTATION PAGE

Form Approved
OMB No. 0704-0188

1. REPORT DATE *(DD-MM-YYYY)*	**2. REPORT TYPE**	**3. DATES COVERED** *(From - To)*
03-02-2014	Memorandum Report	2009 – 2011

4. TITLE AND SUBTITLE

Aerolization During Boron Nanoparticle Multi-Component Fuel Group Burning Studies

5a. CONTRACT NUMBER
N001413WX20872

5b. GRANT NUMBER

5c. PROGRAM ELEMENT NUMBER

6. AUTHOR(S)

Joseph P. Smith, Michael T. Montgomery, Stephen M. Masutani,* Brandon A. Yoza,* Ryan Kurasaki,* Christopher Kinoshita,* and Richard B. Coffin

5d. PROJECT NUMBER

5e. TASK NUMBER

5f. WORK UNIT NUMBER

7. PERFORMING ORGANIZATION NAME(S) AND ADDRESS(ES)

Naval Research Laboratory, Code 6114
4555 Overlook Avenue, SW
Washington, DC 20375-5320

University of Hawaii
2500 Campus Road
Honolulu, HI 96822

8. PERFORMING ORGANIZATION REPORT NUMBER

NRL/MR/6110--14-9506

9. SPONSORING / MONITORING AGENCY NAME(S) AND ADDRESS(ES)

Office of Naval Research
875 N. Randolph Street, Suite 1425
Arlington, VA 22203-1995

10. SPONSOR / MONITOR'S ACRONYM(S)
ONR

11. SPONSOR / MONITOR'S REPORT NUMBER(S)

12. DISTRIBUTION / AVAILABILITY STATEMENT
Approved for public release; distribution is unlimited.

13. SUPPLEMENTARY NOTES
*University of Hawaii, 2500 Campus Road, Honolulu, HI 96822

14. ABSTRACT

A complement to the development of new fuels to meet future energy demands of the U.S. Navy is the enhancement of energy density of existing fuels, thus increasing system payloads, ranges, and/or performance. Addition of energetic solid phase materials, such as boron, magnesium, or aluminum, to liquid hydrocarbon-based fuels can potentially increase energy density. Previous studies investigating the effect of energetic metal addition to liquid hydrocarbon-based fuels have produced mixed results. Boron has excellent potential as a liquid fuel additive due to its high volumetric and gravimetric heating value. Boron carbide (B4C) is widely available due to its commercial application as an abrasive. Boron particles were first tested as fuel additives in the 1950s to 1970s during rocket development and found to significantly increase fuel energy density but boron slurry combustion has problems with ignition, flame stability, and burnout. Recent advances in nanotechnology may allow for high-volume production of boron nanoparticles coated with catalysts and organics to enhance and control combustion, promote suspension and dispersion in fuel, and inhibit premature oxidation. Controlled studies on the effect of boron nanoparticle addition on fuel aerosol droplet size during group burning experiments were conducted by the U.S. Naval Research Laboratory (NRL Code 6114) and the Hawaii Natural Energy Institute (HNEI) at the University of Hawaii (UH) from 2009 to 2011. These studies were performed using a benchtop fuel burner assembly system with a Phase-Doppler-Particle Analyzer (PDPA) to investigate the effect of specific nanoparticle addition (boron, CeO_2-coated boron, and CeO_2) on aerosol droplet size and velocity in a JP-5 carrier fuel. Results of this study showed little to no effect of boron nanoparticle addition (~2.5% weight loading) on aerosol droplet size and velocity distribution fields in the wet, or no flame, condition. Results did suggest an effect of boron nanoparticle addition in the flame case. Rate of change in average droplet diameter with distance from the flame base was greater in the presence of boron nanoparticles, suggesting enhanced combustion and increased droplet evaporation in the JP-5 carrier fuel. Additionally, there was a measureable increase in average droplet velocity near the flame base. However, the opposite effect was a measureable increase in average droplet velocity near the flame base. However, the opposite effect was seen when reduced CeO_2 was used as a catalyst or catalyst only was added to JP-5, suggesting combustion was inhibited.

15. SUBJECT TERMS
Tactical missions Gas turbines Energy enhancement

16. SECURITY CLASSIFICATION OF:			**17. LIMITATION OF ABSTRACT**	**18. NUMBER OF PAGES**	**19a. NAME OF RESPONSIBLE PERSON**
a. REPORT	**b. ABSTRACT**	**c. THIS PAGE**			Richard B. Coffin
Unclassified Unlimited	Unclassified Unlimited	Unclassified Unlimited	Unclassified Unlimited	35	**19b. TELEPHONE NUMBER** *(include area code)* (202) 767-0065

Standard Form 298 (Rev. 8-98)
Prescribed by ANSI Std. Z39.18

DISCLAIMER

TABLE OF CONTENTS

Summary …… 1

Objectives …… 2

Background ……..…… 3

Materials and Methods …….. 4

Results and Discussions …….. 6

Conclusions …….. 12

Literature Cited …….. 12

TABLE OF FIGURES

Figure 1. Theoretical Volume Energy Density Ratio (relative to JP-8) of JP-8 plus additive fuel slurries (Al, graphite, B, B_4C) at different Volume Loadings (0-30%) (Scott Anderson, University of Utah). …… 14

Figure 2. Photograph of group burning facility showing benchtop flat flame burner unit with injector nozzle, variable fuel and gas supply, and Aerometrics Phase-Doppler-Particle Analyzer (PDPA). …… 14

Figure 3. Schematic diagram of the group burning facility. …… 15

Figure 4. Cross-sectional view of the burner assembly. …… 15

Figure 5. Photograph of the (**A**) burner assembly and (**B**) aerosol generator. 16

Figure 6. Diagram of benchtop flat flame burner unit showing injector nozzle assembly with VOAG orifice, fuel and gas supply showing optimal control flame rates, adjustable stage, and Aerometrics Phase-Doppler-Particle Analyzer (PDPA). Position 1, 2, 3, and 4 were fixed stage heights used during initial phase of this study. ……. 16

Figure 7. Control flame using JP-at 2.5 x 10^{-3} cm/sec (JP-5 syringe injection speed); 8.5 L/min carrier gas (air) flow rate; 1.0 L/min shroud gas (methane) flow rate (shown with 20 μm injection orifice). ……. 17

Figure 8. Droplet size and velocity plots at each stage height for JP-5 only F and W runs. ……. 18

Figure 9. Droplet size and velocity plots at each stage height for the Mix 1 F and W runs. Note: Mix 1 W run at the 23 ¼" stage height was not conducted. …… 19

Figure 10. Droplet size and velocity plots at each stage height for Mix 2 F runs. Note: Mix 2 W runs were not conducted. …… 20

Figure 11. Droplet size and velocity plots at each stage height for Mix 3 F and W runs. …….. 21

Figure 12. Droplet size and velocity plots at each stage height for Mix 4 F and W runs. …….. 22

Figure 13. Droplet size and velocity plots for W runs at each stage height.….. 23

Figure 14. Average droplet size and velocity trends for W runs over measured stage heights. ……. 24

Figure 15. Droplet size and velocity plots for F runs at each stage height. …. 25

Figure 16. Average droplet size and velocity trends for F runs over stage heights. ……. 26

Figure 17. Photograph of a H_2/O_2/Ar + EtOH + boron-nanoparticle flame…... 27

Figure 18. Close-up photograph of graduated cylinder containing boron-nanoparticle, JP-5 fuel slurry at ~2.5% loading during settling experiment. …… 27

Figure 19. (**A**) Microscope photograph looking through the 100 μm VOAG orifice that clogged against a counting plate grid spacing of 50 μm. (**B**) Microscope photograph of a 1% w/v CeO_2 (w/ oleic acid) + JP-5 slurry against a counting plate grid spacing of 50 μm. Note: White-dashed circle indicates approximate diameter of 100 μm VOAG orifice.……..… 28

Figure 20. (**A**) Microscope photograph of a 1% w/v boron (w/ oleic acid) + JP-5 slurry against a counting plate grid spacing of 50 μm. (**B**) Microscope photograph showing same 1% w/v boron (w/ oleic acid) + JP-5 slurry under higher magnification. Note: White-dashed circle indicates approximate diameter of 100 μm VOAG orifice. …… 28

Figure 21. (**A**) Microscope photograph of a 0.1% w/v boron (w/ oleic acid) + JP-5 slurry against a counting plate grid spacing of 50 μm. (**B**) Microscope photograph showing same 0.1% w/v boron (w/ oleic acid) + JP-5 slurry under higher magnification. Note: White-dashed circle indicates approximate diameter of 100 μm VOAG orifice. …… 29

TABLE OF TABLES

Table 1. Fuel mixtures tested. ……. 17

Table 2. Summary of droplet size and velocity data for the JP-5 only F and W runs. …… 18

Table 3. Summary of droplet size and velocity data for Mix 1 F and W runs. Note: Mix 1 W run at the 23 ¼" stage height was not conducted. …… 19

Table 4. Summary of droplet size and velocity data for Mix 2 F runs. Note: Mix 2 W runs were not conducted. …… 20

Table 5. Summary of droplet size and velocity data for Mix 3 F and W runs. …… 21

Table 6. Summary of droplet size and velocity data for Mix 4 F and W runs…….. 22

SUMMARY

A complement to the development of new fuels to meet future energy demands of the U.S. Navy is the enhancement of energy density of existing fuels, thus increasing system payloads, ranges, and/or performance. Addition of energetic solid phase materials, such as boron, magnesium, or aluminum, to liquid hydrocarbon-based fuels can potentially increase energy density. Previous studies investigating the effect of energetic metal addition to liquid hydrocarbon-based fuels have produced mixed results (Morris et al., 1955; Faeth, 1984).

Boron has excellent potential as a liquid fuel additive due to its high volumetric and gravimetric heating value. Boron Carbide (B_4C) is widely available due to its commercial application as an abrasive. Boron particles were first tested as fuel additives in the 1950-1970's during rocket development and found to significantly increase fuel energy density but boron slurry combustion has problems with ignition, flame stability, and burnout (Morris et al., 1955; King, 1972; Faeth, 1984; Ulas et al., 2001). Another major obstacle to the application of boron-enhanced fuels is formation of high-melting-point oxides on the particle surface that inhibit further reaction (King, 1972).

Recent advances in nano-technology may allow for high-volume production of boron nanoparticles coated with catalysts and organics to enhance and control combustion, promote suspension and dispersion in fuel and inhibit premature oxidation (Van Devener et al., 2009; Gan and Qiao, 2011; Gan et al., 2012). These advances may spur development of a nanoparticle-hydrocarbon composite fuel slurry where "fuel-soluble" boron nanoparticles undergo controlled combustion at high temperatures enhancing combustion of the hydrocarbon carrier fuel and increasing overall energy density of the multi-component fuel mixture. Boron nanoparticle-doped multi-component hydrocarbon fuels represent a potential high-efficiency, tactical fuel to support future Navy missions at significant future cost-savings to the Navy. Before pilot -scale combustion tests can be conducted, fundamental studies on the effect of boron nanoparticle addition on fuel atomization and aerosolization are required.

Controlled studies on the effect of boron nanoparticle addition on fuel aerosol droplet size during group burning experiments were conducted by the U.S. Naval Research Laboratory (NRL Code 6114) and the Hawaii Natural Energy Institute (HNEI) at the University of Hawaii (UH) from 2009-2011. These studies were performed using a benchtop fuel burner assembly system with a Phase-Doppler-Particle Analyzer (PDPA) to investigate the effect of specific nanoparticle addition (boron, CeO_2-coated boron, and CeO_2) on aerosol droplet size and velocity in a JP-5 carrier fuel. Results of this study showed little to no effect of boron nanoparticle addition (~ 2.5 % weight loading) on aerosol droplet size and velocity distribution fields in the wet, or no flame, condition. Results did suggest an effect of boron nanoparticle addition in the flame case. Rate of change in average droplet diameter with distance from the flame base was greater in the presence of boron nanoparticles, suggesting enhanced combustion and increased droplet evaporation in the JP-5 carrier fuel. Additionally, there was a measureable increase in average droplet velocity near the flame base. However, the opposite effect was seen when reduced CeO_2 was used as a catalyst or catalyst only was added to JP-5 suggesting combustion was inhibited.

Results were initially promising but issues with particle aggregation and agglomeration during follow-on fuel atomization and aerosolization experiments, even at low concentrations, resulted in clogging of the 100 μm diameter oscillating orifice used on the burner assembly in this study. Examination of the mixed-component fuel slurries with a microscope revealed large

Manuscript approved September 17, 2013.

agglomerates of particles in boron and CeO_2-coated boron slurries, but not in the CeO_2 slurries. Tendency of boron-nanoparticles to form agglomerates in liquid hydrocarbon fuels may represent a serious issue that urgently needs to be addressed and resolved in follow-on studies to investigate the feasibility of nanoparticle-enhanced tactical fuels.

OBJECTIVES

Several key technical issues need to be addressed to assess viability of using boron nanoparticle-hydrocarbon multi-component fuel mixtures in modern gas turbine systems. A collaborative research program between the U. S. Naval Research Laboratory (NRL Code 6114), U. S. Naval Academy (USNA), University of Utah, University of Hawaii (UH), Louisiana State University (LSU), and General Electric Corporation (GE) was established to develop a stable, high-energy nanoparticle-hydrocarbon composite tactical fuel. The premise of the proposed effort is the use of Oleic Acid-coated Boron (or B_4C) nanoparticles with a Cerium Oxide (CeO_2) catalyst to enhance energy density of conventional aviation fuels, such as JP-5 and JP-8, for use in gas turbine engines.

Technical objectives of this program include:

1. Particle production and characterization
2. Cost effective and high volume production of 50-200 nm nanoparticles in fuel
    a) Achieve a stable and uniform suspension of particles in fuel
    b) Achieve acceptable mixture properties (viscosity)
    c) Demonstrate acceptable flow and atomization through engine fuel injector
    d) Demonstrate no harm to the fuel distribution system
3. Ignition and combustion of fuel mixture
    a) Achieve combustion and ignition at gas turbine conditions within residence time of current combustion systems
    b) Demonstrate heat release from solid fuel
4. Maintain engine reliability and life
    a) Demonstrate minimal levels of deposits/erosion/corrosion of components downstream of combustion chamber
5. Meet Health & Safety and Observability requirements
    a) Verify product species composition
    b) Assess hazard and handling requirements of products

Before pilot and full-scale combustion tests can be conducted to assess viability of utilizing high-energy nanoparticle-hydrocarbon composite fuel, fundamental data on single and group droplet burning, and atomization phenomena are required (Technical Objective 2 a-d). Toward this end, experiments were conducted with NRL Code 6114 at the Hawaii Natural Energy Institute (HNEI) at (UH) at benchtop scale. Results are intended to complement potential larger-scale combustion tests to be conducted in more complex environments at LSU (swirl-stabilized combustion) and at GE and USNA (full-scale gas turbine combustion).

Three specific categories of benchtop experiments were performed by NRL and UH using existing facilities and instrumentation at HNEI: 1) atomization/aerosolization studies of

multi-component fuel; 2) single droplet combustion tests; and 3) combustion of dilute ensembles of droplets to examine group burning phenomena. Initial comparison of single droplet burning rates of conventional JP fuel and multi-component fuel were performed by UH HNEI using a suspended droplet test configuration and group burning phenomena were also investigated.

BACKGROUND

Global energy availability is reaching a state where the U.S. Navy needs to consider new energy policies, technologies, and alternate fuels in its strategic planning to meet future needs. Some alternate fuels and new technologies being considered include biofuels, synthetic fuel designs, and hydrogen fuel cells. Although these new energy sources have great potential to partially meet private and industrial sector energy demands, they have limited utility in supporting military fuel requirements. Biofuels, specifically bio-diesel, can be costly to produce and have lower energy yield and combustion efficiency than current military aviation fuels such as JP-5, 7, and 8. Use of bio-diesel based fuels in military aviation applications could reduce range, limit performance, and lower maximum payload of military aircraft thereby reducing mission capability. In addition, biofuels can degrade during long term storage, changing fuel molecular composition that could further reduce fuel energy (Leung et al., 2006). Development of synthetic fuels and biofuels is not guaranteed to meet future energy demand of the U. S. Navy and these fuels will likely be expensive.

An alternative to new fuel development for use in Navy air, land, and sea tactical systems is increasing energy density of existing fuels thus increasing system payloads, ranges, and/or performance. Advanced synthetic hydrocarbon fuels such as JP-10 have volumetric energy densities ~15% above that for JP-8 (34.2 MJ/liter). But further significant increases in energy density of synthetic hydrocarbon based fuels are unlikely. Addition of energetic solid phase materials such as boron, magnesium, or aluminum to liquid hydrocarbon-based fuels can potentially increase energy density. Previous studies to investigate the effect of additions of energetic metals to liquid hydrocarbon-based fuels have produced mixed results (Morris et al., 1955; Faeth, 1984).

Boron is particularly attractive as a potential aviation fuel additive. It has an exceptionally high combustion energy resulting in a high volumetric and gravimetric heating value and its properties allow for safe handling and storage. This high combustion energy density can theoretically increase the gravimetric energy density of hydrocarbon fuels such as JP-8 as high as 135.8 MJ/liter from 34.2 MJ/liter if added as pure Boron at 30% volume loading. Boron Carbide (B_4C) can theoretically increase energy density of JP-8 up to 129.4 MJ/liter at the same volume loading (**Fig. 1**). Boron Carbide is widely available due to its commercial application as an abrasive.

Boron particles were first tested as fuel additives in the 1950-1970's during rocket development and found to significantly increase fuel energy density but the specific energy yield of the fuel was unstable during ignition (King, 1972). Greater than micron-sized energetic metal particles do not always remain suspended homogeneously in fuel mixtures. Rate of particle combustion is often uncontrolled, resulting in "microexplosions" (Wong et al, 1992; 1994; Gan and Qiao, 2011; Gan et al., 2012). Investigations of boron slurry combustion have reported problems with ignition, flame stability, and burnout (King, 1972; Faeth, 1984; Ulas et al., 2001; Gan and Qiao, 2011; Gan et al., 2012). Another major obstacle to application of boron-enhanced

fuels is formation of high-melting-point oxides on the particle surface that inhibit further reaction (King, 1972).

Recent advances in nano-technology have the potential to produce high-volumes of boron nanoparticles coated with catalysts and organics to enhance and control combustion, promote suspension and dispersion in the fuel and inhibit premature oxidation (Van Devener et al., 2009; Gan and Qiao, 2011; Gan et al., 2012). These advances may help develop a nanoparticle-hydrocarbon composite fuel slurry where "fuel-soluble" boron nanoparticles undergo controlled combustion at high temperatures, enhancing combustion of the hydrocarbon carrier fuel, and increasing overall energy density of multi-component fuel mixtures.

If issues related to particle miscibility, ignition, flame stability, and burn rate can be addressed, Boron nanoparticle-doped multi-component hydrocarbon fuels represent a potential high-efficiency, tactical fuel that could increase thrust to weight ratio, reduce propulsion system size, and/or increase ranges (engine can go a longer distance for the same amount of fuel) all at significant future cost-savings to the Navy. Before pilot and full-scale combustion tests can be conducted to assess viability of utilizing such fuel mixtures, fundamental studies on the effect of boron nanoparticle addition on fuel atomization and aerosolization are required. The results of atomization/aerosolization studies of multi-component fuel slurries conducted by NRL Code 6114 and UH at HNEI from 2009-2011 presented in this report are a first step in addressing these issues.

MATERIALS AND METHODS

Multi-component fuel slurry atomization/aerosolization studies were conducted using the group droplet burning facility at HNEI. The group droplet burning facility consists of a benchtop-scale burner mounted on a manual translation stage, variable fuel and gas supply rates, and injector nozzles that can be configured to investigate diffusion and premixed flames (**Fig. 2 & 3**). Liquid fuel droplets are generated using a vibrating orifice aerosol generator (VOAG) manufactured by TSI (model 3450). The vibrating orifice produces a nearly-monodispersed stream of droplets which are advected into the burner through an injector nozzle using a carrier gas. The size of the replaceable VOAG orifice determines initial droplets diameter; in the present experiments, tested diameters ranged from about 20 μm to 100 μm.

Liquid fuel is fed from a stepper motor-driven syringe pump to the VOAG orifice at a constant programmable rate (0.001 - 2.2 cm^3/min). A piezoelectric transducer vibrates the orifice at a selected frequency, producing a uniform vertical stream of droplets that are advected into the burner plenum above the aerosol generator and through a contraction and injector tube into the combustion zone. An additional shroud gas outside the flame base can be used as an ignition source. The carrier gas and shroud gas used in initial studies were air and methane, respectively. No shroud pilot flame was employed in follow-on studies. Mass flow controllers supply research grade gases (>99.99% purity) to the VOAG and burner from compressed gas cylinders. The inert gas and fuel mass flow controllers have an operating range of 0 – 50 L/min; the oxidizer mass flow controller has an operating range of 0 – 10 L/min. A system to pre-vaporize the liquid fuel and add that vapor to the droplet feedstream was constructed but was not employed in these experiments.

The modular burners can be assembled in different configurations to investigate diffusion and pre-mixed flames of liquid and/or gaseous fuels in air or O_2. Various diluents can be added

to the fuel or oxidizer streams. **Figure 4** presents a cross section of the assembled burner that shows the flow paths of the different reactants and inert gases. **Figures 5A & 5B** are photographs showing details of the burner and aerosol generator. Two geometries are available with fuel jet exit diameters of 0.305 (7.7 mm) and 0.875 (22 mm) inches.

The droplet generator/burner assembly is mounted on a two-dimensional (vertical and radial) manual translation stage. The range of travel is in excess of 30 cm vertically and 15 cm radially. The burner stage can be raised or lowered to allow for fixed point measurements of aerosol spray and flame parameters relative to the burner base.

The spatial evolution of the size distribution of the initially near-monodispersed droplets provides insight into the burning process and rates. Measurements of aerosol droplet size and velocity were made using an Aerometrics Phase-Doppler-Particle Analyzer (PDPA). PDPA measurements are performed using a small, non-intrusive optical probe volume defined by the intersection of two laser beams and the image of a spatial filter that limits the field of view of the optical detectors. Interference of the two beams creates a fringe pattern within the probe volume. As a droplet passes through the moving fringe induced by a Bragg cell to avoid directional ambiguities, it scatters light that is collected by a receiving lens that projects a portion of the scattered light onto three photodetectors located at slightly different angles from the probe volume. Each detector produces a Doppler burst signal with a frequency proportional to the particle velocity. Phase shift between the Doppler burst signals from two different detectors is proportional to the spherical droplet size. Two different pairs of detectors (three detectors total) were used to reduce ambiguities that might occur when the droplet size range is large. A Real-time Signal Analyzer (RSA) and personal computer was used to process the Doppler signals from the photodetectors using a discrete Fourier transform method.

Different sets of optics were available to accommodate a broad range of droplet sizes and velocities. The instrument was typically configured to perform 60° off-axis forward scattering employing a 1000 mm fl transmitting lens and 500 mm fl receiving lens. The 514.5 nm line of a 500 mW (all lines) Ar-ion water-cooled laser was employed to perform simultaneous measurements of droplet size and a single component (axial; streamwise) of velocity.

Atomization/aerosolization studies determined the effect of nano-particle loadings (and particle sizes) in fuel (JP-5 or other proxy fluid) on droplet size and velocity distributions under fixed nozzle operating parameters (**Fig. 6**). Different fuel injection pressures and gas flow rates were tested to determine the optimal control flame for conducting atomization studies using JP-5 as the control fuel. Optimal parameters were arbitrarily determined as the settings that provided a consistently stable flame height and shape. **Figure 7** shows a control flame with the following settings: 2.5×10^{-3} cm/sec JP-5 syringe injection velocity; 8.5 L/min carrier gas (air) flow; 1.0 L/min shroud gas (methane) flow.

Nanoparticle additives used in this study have a core of a high energy density material (boron or B_4C). Boron nanoparticles were prepared at the Department of Chemistry, University of Utah using methods developed by Dr. Scott Anderson. In brief, commercial boron powder, a small amount of organic coating/solubilizing agent (oleic acid, $C_{18}H_{34}O_2$), and CeO_2 catalyst (CeO_2 or reduced CeO_2, ~100 nm powder, if used) were milled together in a tungsten carbide ball-mil with hexane to wet the particle surfaces. The CeO_2 catalyst was added to some nanoparticles (1g CeO_2 per 10 g B) to accelerate ignition and control combustion rate of boron in the hydrocarbon carrier fuel. Oleic acid was used to coat particles to increase their solubility in carrier fuel and to reduce premature oxidation during storage. Particles were milled in argon atmosphere to avoid oxide formation. Particles with nominal sizes ranging from ~50 to > 300

nm can be produced, with size controlled by milling time. X-ray photoelectron spectroscopy measurements on boron nanoparticle batches detected cerium boride indicating that the CeO_2 chemically bonds to the boron. Sample batches with mean particle sizes ranging from 40 nm to 250 nm were produced, as determined by a dynamic light scattering (DLS) technique at University of Utah.

Large, micron-sized or uncoated particles can settle out of solution within seconds, whereas coated nanoparticles form suspensions of particles stable for weeks in JP-5 and other hydrocarbons. An intermediate settling or filtration step removed micron-sized or uncoated particles prior to final volume dilution in JP-5 and shipment from the University of Utah to HNEI. Once at HNEI nanoparticle/fuel mixtures were sonicated for 1 - 24 hours prior to use. Examples of different fuel mixtures tested in this study are listed in **Table 1**.

For the 2009 aerosolization/atomization studies, JP-5 control fuel and fuel mixtures with different nanoparticle loadings (and particle sizes) were run through the burner assembly system under both flame (F) and wet, no flame (W) conditions. During each run, aerosol droplet size and velocity were measured at four different fixed stage height positions (23 ¼", 21 ¾", 20 ¼", 19") using the PDPA (**Fig. 6**). The fuel burner system was rinsed with 2-propanol after each even run. Individual run results were compiled by fuel mixture type, flame condition (F or W), and stage height. Droplet size data were binned into 5 μm bins and velocity data were binned into 0.5 m/sec bins. Follow on studies were conducted in 2010 and 2011 using similar experiment controls with different nano-particulate loadings.

A total of five types of liquid fuels and slurries were tested: 1) JP-5; 2) pure alcohols; 3) dilute slurries of boron nanoparticles in either JP-5 or alcohol; 4) dilute slurries of CeO_2 coated boron nanoparticles in either JP-5 or alcohol; and 5) dilute slurries of CeO_2 in either JP-5 or alcohol. Sealed one-gallon pails of JP-5 fuel were obtained from the Pearl Harbor Naval facility. Three alcohols were employed: ethanol (C_2H_6O), methanol (CH_4O), and 2-propanol (C_3H_8O). Methanol and 2-propanol had purities of 99.9%; ethanol purity was 99.98%.

RESULTS AND DISCUSSION

Initial Fuel Aerosolization/Atomization Experiments

Initial fuel aerosolization/atomization studies were conducted in March 2009. In order to establish and maintain a running baseline droplet size (diameter) and velocity distribution for the burner assembly system runs using JP-5 only were conducted prior to and in between runs using different fuel mixtures. **Table 2** shows a summary of droplet size and velocity results for each flame condition (F and W) and stage height for JP-5 only runs. In general, for baseline W runs, average droplet diameter tends to stay constant with decreasing stage height whereas average droplet diameter tends to decrease with decreasing stage height for F runs. This makes sense since during combustion droplets shrink as the liquid fuel vaporizes due to heat transfer from the flame. This vapor burns homogeneously in the gas phase at loci where appropriate concentrations of oxidizer exist.

A different trend can be seen in average droplet velocity which decreases with decreasing stage height for W runs and potentially increasing (with the exception of the 19" stage height case) with decreasing stage height for F runs. These trends are generally as expected. As stage height decreases, PDPA is measuring droplets that are further away from the burner base , or

flame base in F runs. In W runs, droplets slowed as they left the nozzle. During F runs, as droplets leave the base of the flame, they are combusted and rapidly evaporated, decreasing droplet diameter and increasing droplet velocity until they reach significant distance from the flame base for combustion and evaporation to slow.

Figure 8 shows plots of droplet size and velocity at each stage height for the JP-5 only F and W runs. The reason for the bi-(or-multi) modality in distribution of droplet size and velocity for some of these runs (e.g. droplet size for F run at 23 ¼"), and some of the fuel mixtures, is unknown. This may be some function of true size and velocity distribution, an artifact of the burner system and PDPA set-up, or could possibly be due to problems with clogging of the oscillating orifice in the burner assembly during many of the fuel mix runs. In general, plots for the JP-5 only runs show a broadening of droplet size distribution with decreasing stage height in both the F and W cases, with a clear shift towards smaller droplet diameters for F runs and potentially a shift towards larger droplet diameters for W runs. Droplet velocity distribution narrows with decreasing stage height and shift towards lower velocities in the W runs. There is potentially a shift in droplet velocity distribution with decreasing stage height towards lower velocities in F runs but there is also a broadening of the distribution which makes any conclusion difficult.

Fuel Mixture 1 contained boron nanoparticles with an oleic acid coating in JP-5 at an approximate mass loading of 2.4% (**Table 1**). **Table 3** shows a summary of droplet size and velocity results for each flame condition (F and W) and stage height for the Mixture 1 runs. Mixture 1 W runs at the 23 ¼" stage height were not conducted. Average droplet diameter is near constant with decreasing stage height for the W runs but the 20 ¼" stage height results show an abnormally low average droplet diameter. The reason for the low average diameter is not known and these data are suspect. Once again, there may have been problems with clogging of the oscillating orifice in the burner assembly. Average droplet diameter for Mixture 1 F runs, however, shows the same clear trend of decreasing diameter with decreasing stage height as seen in JP-5 only F runs. And, like the JP-5 only runs, average droplet velocity clearly decreases with decreasing stage height for Mixture 1 W runs. Average droplet velocity for Mixture 1 F runs appears to remain relatively constant at each stage height, except there is the same sharp decrease for the 19" stage height as seen with JP-5 only runs.

Droplet size was compared with velocity at each stage height for Mixture 1 F and W (**Fig. 9)**. At least for the Mixture 1 F runs, droplet size and velocity distribution over the 4 stage heights is similar to that for JP-5 only, albeit with a significantly higher average droplet diameter and a slightly higher average droplet velocity. Droplet velocity distribution for Mixture 1 W again shows a clear narrowing in droplet velocity distribution with decreasing stage height and shift towards lower velocities. There is little that can be concluded from droplet size distribution with decreasing stage height for Mixture 1 W due to the missing 23 ¼" stage height data and questionable 20 ¼" stage height data, potentially caused by problems with clogging of the oscillating orifice.

Fuel Mixture 2 contained boron nanoparticles with a reduced CeO_2 and oleic acid coating in JP-5 at an approximate mass loading of 2.5% (**Table 1**). **Table 4** shows a summary of droplet size compared to velocity for the F flame condition at each stage height for Mixture 2. Mixture 2 W runs were not conducted. Average droplet diameter for Mixture 2 F generally decreased with decreasing stage height. Average droplet velocity for Mixture 2 F at each stage height varied between 3.04 to 3.79 m/sec. The same sharp decrease for the 19" stage height in the JP-5 only

and Mixture 1 F runs is not apparent. Both average droplet size and velocity seems to be closer to the values for the JP-5 only baseline than Mixture 1.

Plots of droplet size and velocity at each stage height for the Mixture 2 F runs are shown in **Figure 10**. As with the JP-5 only and Mixture 1 F runs, the droplet size distribution for the Mixture 2 F runs shows a broadening with decreasing stage height but the shift towards smaller diameters is not as clear. In the Mixture 2 F runs, however, there is no clear trend or shift in the droplet velocity distribution with changing stage heights.

Fuel Mixture 3 contained boron nanoparticles with a CeO_2 and oleic acid coating in JP-5 at an approximate mass loading of 2.5% (**Table 1**). **Table 5** shows a summary of droplet size and velocity results for each flame condition (F and W) and stage height for the Mixture 3 runs. Consistent with the JP-5 only baseline and previous Mixture 1 and 2 results, average droplet diameter is generally constant with decreasing stage height for Mixture 3 W and droplet diameter decreases with stage height for Mixture 3 F. The trend in average droplet velocity for Mixture 3 W is also similar to previous experiments, with average velocity decreasing with stage height. Average droplet velocity for Mixture 3 F appears constant at each stage height with a sharp decrease at the 19" stage height.

Plots of droplet size and velocity at each stage height for the Mixture 3 F and W runs are shown in **Figure 11**. Mixture 3 F has similar patterns to previous runs with a broadening of droplet size distribution and a shift towards smaller diameters with decreasing stage height. Droplet size distribution for Mixture 3 F runs appears relatively constant at all stage heights. The same narrowing in droplet velocity distribution with decreasing stage height and shift towards lower velocities with W can be seen. And once again, there is a shift in droplet velocity distribution with decreasing stage height towards lower velocities with F.

Fuel Mixture 4 contained CeO_2 nanoparticles with an oleic acid coating in JP-5 at an approximate mass loading of 2.4% (**Table 1**). **Table 6** shows a summary of droplet size and velocity results for each flame condition (F or W) and stage height for the Mixture 4 runs. As expected, average droplet diameter is generally constant with decreasing stage height for Mixture 4 W and average droplet velocity is decreasing. Interestingly, average droplet diameter is generally constant with decreasing stage height for Mixture 4 F. Mixture 4 is CeO_2 (coated w/ Oleic Acid) in JP-5 in absence of boron nanoparticles. It is possible that, because CeO_2 is added to control boron combustion rate in the JP-5 hydrocarbon carrier fuel, CeO_2 is limiting combustion and/evaporation of aerosol droplets in the flame resulting in a relatively constant droplet size distribution during F runs. This would be consistent with the observation that average droplet velocity for Mixture 4 F runs appears constant at each stage height with no apparent decrease at the 19" stage height.

Plots of droplet size and velocity at each stage height for the Mixture 4 F and W runs are shown in **Figure 12**. The relatively constant droplet size distribution for Mixture 4 F is apparent. Otherwise, all plots show similar distributions as those seen in the JP-5 only baseline F and W.

These initial results suggest that boron nanoparticle addition at low mass loadings (~2.5%) has little effect on fuel atomization/aerosolization. In this study, addition of homogeneously suspended boron (CeO_2 and oleic acid coated) nanoparticle slurry to JP-5 might be expected to have the following impacts on aerosol droplet size and velocity:

1. Wet (W) Case:

a. Droplet Size – Droplet size should remain constant at a given distance from burner face for both JP-5 only and each fuel mixture.
b. Droplet Velocity – Droplet velocity should decrease with distance from burner face at the same rate for both the JP-5 alone and each fuel mixture.

2. Flame (F) Case:

a. Droplet Size – Boron nanoparticles should enhance combustion and increase flame temperatures. Droplet size should decrease more rapidly with increasing distance from the burner face relative to JP-5 alone.
b. Droplet Velocity – Droplet velocity should remain relatively constant or increase with distance from burner face until a critical distance away from flame base.

Droplet size and velocity distributions were similar for all stage heights for JP-5 alone and Mixture 4 (CeO_2 only) (**Fig. 13**). As previously noted, no W runs were performed for Mixture 2, and the 20 1/4" stage height results for Mixture 1 were questionable. There does appear to be a difference in droplet size distribution at all stage heights for Mixture 3 and potentially for Mixture 1. Likewise, the droplet velocity distributions for Mixtures 1 and 3 show subtle difference from the baseline JP-5 alone or Mixture 4. This could indicate an impact of nanoparticulate loading on aerosolization, but problems with clogging of the oscillating orifice in the burner assembly make drawing any clear conclusions difficult.

In general, average droplet size diameter is the same for all W runs and all stage heights, with exception of the questionable results for Mixture 1 (**Fig. 14**). Average droplet velocity was similar between the JP-5 only W baseline run and all Mixtures at each stage height and, as expected, showed a similar rate of decrease with decreasing stage height. These data suggest nanoparticle additions had a minimal impact on aerosol droplet size and velocity distribution.

Droplet size distributions at each stage height show subtle differences between the JP-5 baseline and Mixtures at the 23 ¼", 21 ¾", and 20 ¼" stage heights, especially Mixtures 1 and 3 and, to a lesser degree, Mixture 2 and 4 for F runs (Fig. 15). This could indicate an effect of boron nanoparticle addition on droplet size during combustion, although the skewing of the height distribution towards greater droplet diameter for Mixtures 1 and 3 is interesting. Droplet velocity distributions of JP-5 only F runs and those of different nanoparticle mixtures look strikingly similar at the 21 ¾", 20 ¼", and 19" stage heights, with the only apparent differences appearing at the 23 ¼" stage height. Again, given clogging problems, these results could be an artifact or could be indicative of an effect of boron nanoparticle addition on aerosol droplet velocity distribution field during combustion.

In contrast to W runs, there were notable differences in average droplet diameter at different stage heights during F runs between JP-5 alone and different fuel mixtures and also among different fuel mixtures (**Fig. 16**). But, it is the different rate of change in the average droplet diameter with decreasing stage height, or increased distance from the flame base, that is most striking. For JP-5 alone F baseline, average droplet diameter decreased at a rate of -4.2 μm/inch. Decrease in average droplet diameter for Mixtures 1 and 3 were -5.2 and -7.1 μm/inch, respectively. Large standard deviations in these data, compounded by problems with clogging, make interpretation problematic but these results tend to support the conclusion that boron nanoparticle addition to JP-5, with or without a CeO_2 catalyst, may increase combustion

temperatures in carrier fuel, thus affecting droplet evaporation rates. Note that the same difference in decrease rate was not seen for Mixtures 2 and 4 F (-1.3 and +0.5 μm/inch, respectively). Mixture 2 used a reduced CeO_2 catalyst with boron nanoparticles and Mixture 4 was CeO_2 only with no boron nanoparticles. As compared to JP-5 alone and Mixtures 1 and 3, these mixtures may have had the opposite effect and inhibited combustion of JP-5.

Looking at average droplet velocity, there were differences between the JP-5 alone and fuel mixtures at the stage heights closest to the flame base (23 ¼") and furthest away from the flame base (19"). Mixtures 1 and 3 show in increase in average droplet velocity closest to the flame base (23 ¼") when compared to JP-5 alone. This again could indicate enhanced combustion due to the addition of the boron nanoparticles. Average droplet velocity for Mixtures 2 and 4 F increased at stage heights furthest away from the flame base (19") though the cause is unknown.

Follow-on Fuel Aerosolization/Atomization and Group Burning Experiments

Follow-on, fuel aerosolization/atomization and group burning experiments were conducted in 2010-2011. As stated earlier, results of group burning experiments will be reported separately by UH/HNEI and reference here only as necessary. For follow-on studies, a series of experiments using different fuel slurry mixtures (boron, CeO_2, reduced CeO_2), different nanoparticle loadings (0.5% - 10% w/v), and different carrier fuels (JP-5, ethanol (C_2H_6O), methanol (CH_4O), and 2-propanol (C_3H_8O)) were planned. A mixture of $H_2 + O_2$ reaction was used as a pilot flame for droplet combustion and argon was the carrier gas for liquid droplets produced by the VOAG.

Attempts to consistently burn nanoparticle fuel slurries, however, were unsuccessful. For each run, particles quickly clogged the orifice of the aerosol generator. **Figure 17** shows an example of a flame for a boron-nanoparticle mixture in ethanol. The green emission characteristic of boron oxidation (i.e., probably electronically excited BO_2) can be seen clearly (Yuasa & Isoda, 1991; Young et al., 2009). High luminosity of the JP-5 flames obscures this green emission, although it is visible to the eye during experiments but does not appear clearly in video or photographs. Continued combustion of particles or droplets near the flame top can also be seen clearly. The orifice of the aerosol generator clogged shortly after this photograph was taken. Clogging continued even after increasing orifice diameter to 100 μm and diluting nanoparticle fuel slurries from ~10% w/v to 0.5%. Additional sonification of up to 24 hrs to disperse nanoparticles did not resolve the clogging problem.

Some clogging had occurred in the initial aerosolization/atomization experiments but not to the degree experienced in follow-on studies. Pre-milled nanoparticle/fuel mixtures received from the University of Utah had been stored for about ten months prior to use in these experiments during repairs and modifications to the UH/HNEI experimental facility. CeO_2 nanoparticles (that did not clog the orifice) also had been stored for the same period under the same conditions. Simple settling experiments using graduated cylinders were conducted on pre-sonicated fuel slurries that clearly showed rapid nanoparticle aggregation and/or agglomeration to > μm size particles in the carrier fuel (**Fig. 18**)

Examination of fuel slurries with a microscope revealed large agglomerates of CeO_2-coated and uncoated boron slurries, but not CeO_2 only slurries. After a 12 hour pre-sonification, an optical microscope and a counting plate from a Hausser Scientific Model 3200

hemacytometer was used to visualize the CeO_2 and boron nanoparticle slurries. **Figure 19A** is a magnified microscope photograph looking through the 100 μm VOAG orifice that clogged against a counting plate grid spacing of 50 μm. **Figure 19B** is a photograph of a 1% w/v CeO_2 (w/ oleic acid) + JP-5 slurry against a counting plate grid spacing of 50 μm under similar magnification. The black dots are nanoparticles. Although some agglomeration is apparent, slurry particles appear to be well-mixed in the carrier fuel with nano-to-micron scale diameters.

Figures 20A & 20B show microscope photographs under different magnifications of a 1% w/v boron (w/ oleic acid) + JP-5 slurry against a counting plate grid spacing of 50 μm. The sample is heterogeneously mixed. A high degree of particle agglomeration is apparent, with effective particle-agglomeration sizes on the order of 10-100 microns. The sample was diluted ten-fold to 0.1% w/v to disperse the agglomerates. **Figures 21A & 21B** show microscope photographs under different magnifications of the 0.1% w/v boron (w/ oleic acid) + JP-5 slurry against a counting plate grid spacing of 50 μm. Large agglomerates (> 10 μm) can still be seen clearly. A gentle stream of N_2 gas was directed onto the slide and large particle-agglomerates moved as a unit, rather than deform or fracture, suggesting a degree of adhesion and mechanical stability. Dilute solutions of boron nanoparticles coated with CeO_2 in JP-5 also clogged the VOAG orifice and formed similar agglomerates when observed with the microscope.

The agglomeration of boron nanoparticles in high-density fuel slurries (> 1% w/v) is consistent with results of other workers (Gan et al., 2012). In this study, these large boron-nanoparticle agglomerates resisted dispersion, even after prolonged sonification and/or dilution to lower-density slurries (< 1% w/v). Physiochemical mechanisms for boron nanoparticle agglomeration/aggregation in JP-5 were not investigated in this study, nor were agglomeration/aggregation behavior in different hydrocarbon-fuel matrices. These are areas for future research.

Formation of greater than micron-sized energetic metal particles-agglomerates in liquid fuels would not remain suspended in fuel mixtures and could promote "microexplosions" during combustion and problems with ignition, flame stability, and burnout observed in earlier investigation of energetic particle additions to liquid hydrocarbon-based fuels (King, 1972; Faeth, 1984; Wong et al, 1992; 1994; Ulas et al., 2001; Gan and Qiao, 2011; Gan et al., 2012). Although gas turbine fuel injector orifices are significantly larger than the 100 μm VOAG orifice used in this study, proposed micro-orifice injectors to reduce pollutant emissions are of approximately the same size. Moreover, most commercial fuel systems use filters to trap particulates greater than about 10 μm. These preliminary results suggest particle agglomeration in boron-nanoparticle fuel slurries could pose an operational problem and needs to be taken into consideration when assessing feasibility of nanoparticle-enhanced tactical fuels in the field.

It is important to note that boron-nanoparticle fuel slurries used in the follow-on fuel aerosolization/atomization and group burning experiments were stored for ~ 10-months after milling prior to use. Nanoparticle fuel slurries used in initial fuel aerosolization/atomization experiments had not been stored for an extended period of time. Some clogging of the VOAG orifice was observed during the initial aerosolization/atomization experiments but the VOAG orifice used in these experiments was much smaller in diameter (20 μm to a 35 μm) than the 100 μm VOAG orifice used in the follow-on experiments. This tendency of boron-nanoparticles to form agglomerates over time may represent a serious storage and handling problem that also needs to be addressed when considering nanoparticle-enhanced tactical fuels.

CONCLUSIONS

This report summarizes the results of the fuel aerosolization/atomization experiments conducted from 2009-2011 by the NRL Code 6114 and HNEI at UH using a benchtop fuel burner assembly system with a fixed Phase-Doppler-Particle Analyzer (PDPA) to investigate the effect of boron nanoparticle addition on aerosol droplet size and velocity in a JP-5 carrier fuel. Initial experiment results showed little to no effect of boron nanoparticle addition (~ 2.5 % weight loading) on aerosol droplet size and velocity distribution fields in the wet, or no flame, condition. Results did, however, suggest an effect of boron nanoparticle addition in the flame case. The rate of change in average droplet diameter with distance from the flame base was greater with boron nanoparticles, suggesting enhanced combustion and increased droplet evaporation in JP-5 fuel. Additionally, there may be 0a small increase in average droplet velocity near the flame base. The opposite effect was seen, however, when reduced CeO_2 was used as a catalyst or catalyst only was added to JP-5 suggesting inhibition of combustion.

Results were initially promising but issues with nanoparticle aggregation/agglomeration in follow-on experiments resulted in repeated clogging of the oscillating orifice used on the burner assembly. Particle agglomeration in boron-nanoparticle fuel slurries could pose a serious operational problem and needs to be taken into consideration when assessing the feasibility of employing nanoparticle-enhanced tactical fuels in the field. Furthermore, this tendency of boron-nanoparticles to form agglomerates over time may represent a serious storage and handling problem that also needs to be addressed and resolved in follow-on studies.

LITERATURE CITED

Faeth, G. M. 1984. Status of boron combustion research. Technical Report for Air Force Office of Scientific Research, AFOSR-TR-85-0466.

Gan, Y., and L. Qiao. 2011. Combustion characteristics of fuel droplets with addition of nano and micron-sized aluminum particles. *Combustion and Flame* 158(2): 354-368.

Gan, Y., Y. S. Lim, and L. Qiao. 2012. Combustion of nanofluid fuels with the addition of boron and iron particles at dilute and dense concentrations. *Combustion and Flame* 159: 1732-1740.

King, M. K. 1972. Boron ignition and combustion in air-augmented rocket afterburners. *Combustion Science and Technology* 5(1): 155-164.

Leung, D. Y. C., B. C. P. Koo, and Y. Guo. 2006. Degradation of biodiesel under different storage conditions. *Bioresource Technology* 97(2): 250-256.

Morris, J. F., R. M. Caves and A. M. Lord. 1955. Blow-out velocities of several slurry and liquid fuels in a 1-7/8 inch diameter combustor. NACA Research Memorandum E54L27a. Lewis Flight Propulsion Laboratory, Cleveland, OH.

Ulas, A., K. K. Kuo, and C. Gotzmer. 2001. Ignition and combustion of boron particles in fluorine-containing environments. *Combustion and Flame* 127(1/2): 1935-1957.

Van Devener, B., J., P. L. Perez, J. Jankovich, and S. L. Anderson. 2009. Oxide-Free, Catalyst-Coated, Fuel-Soluble, Air-Stable Boron Nanopowder as Combined Combustion Catalyst and High Energy Density Fuel, *Energy & Fuels* 23: 6111–6120.

Wong, S. C., and A. C. Lin. 1992. Microexplosion mechanisms of aluminum/carbon slurry droplets. *Combustion and Flame* 89: 64-76.

Wong, S. C., A. C. Lin and C. E. Wu. 1994. Microexplosions of boron and boron/carbon slurry droplets. *Combustion and Flame* 96: 304-310.

Young, G., K. Sullivan, M.R. Zachariah, and K. Yu. 2009. Combustion characteristics of boron nanoparticles. *Combustion and Flame* 156(2): 322-333.

Yuasa, S., and H. Isoda. 1991. Ignition and combustion of small boron lumps in an oxygen stream. *Combustion and Flame* 86(3): 216-218.

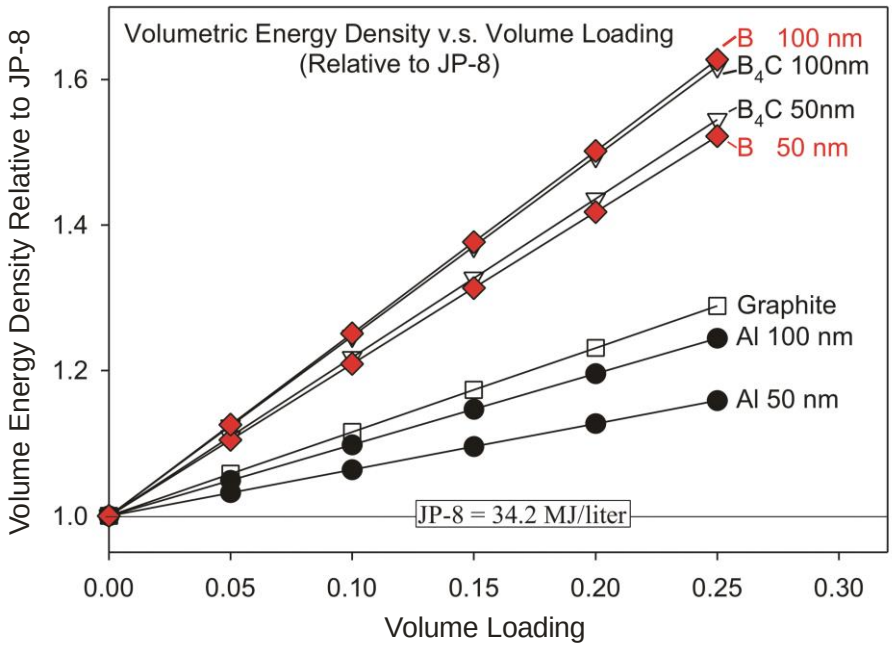

Figure 1. Theoretical Volume Energy Density Ratio (relative to JP-8) of JP-8 plus additive fuel slurries (Al, graphite, B, B_4C) at different Volume Loadings (0-30%) (Scott Anderson, University of Utah).

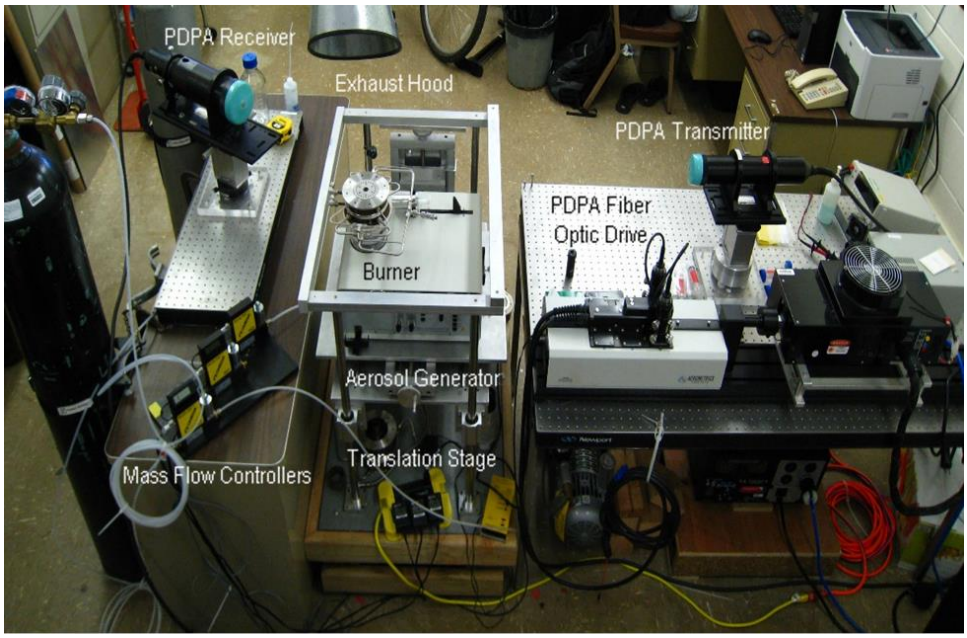

Figure 2. Photograph of group burning facility showing benchtop flat flame burner unit with injector nozzle, variable fuel and gas supply, and Aerometrics Phase-Doppler-Particle Analyzer (PDPA).

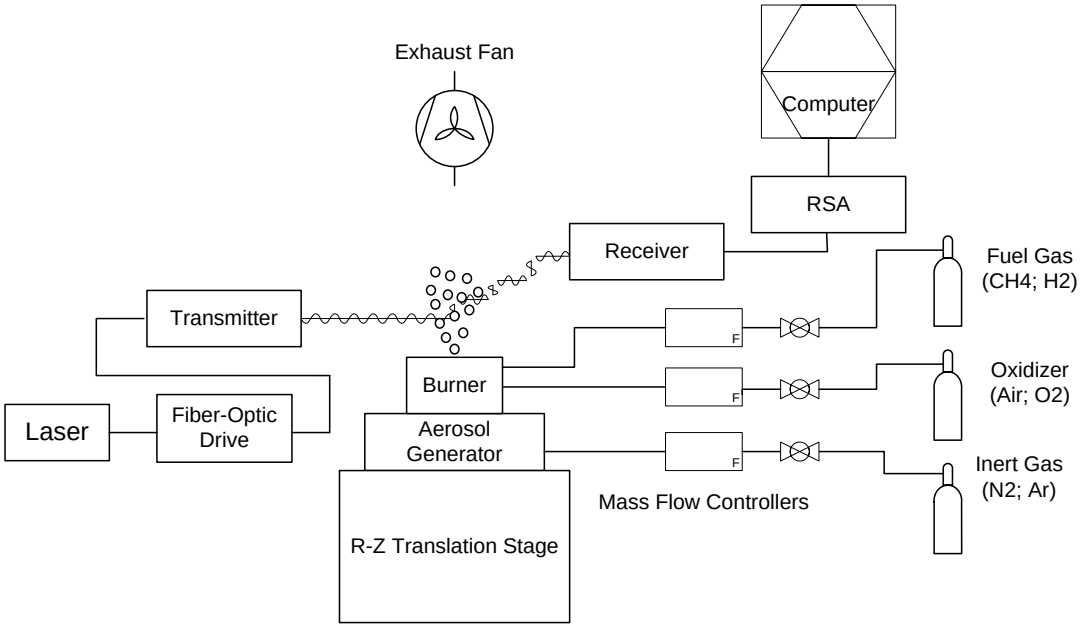

Figure 3. Schematic diagram of the group burning facility.

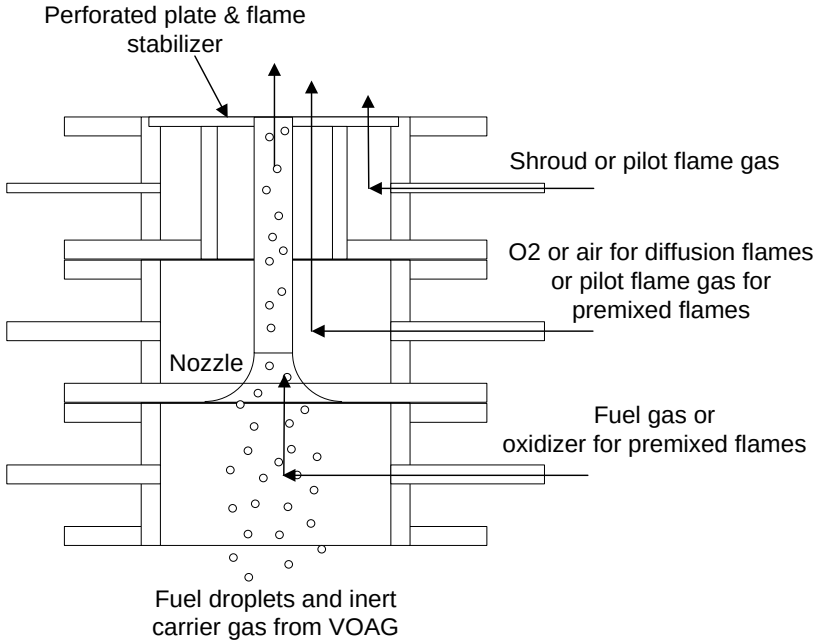

Figure 4. Cross-sectional view of the burner assembly.

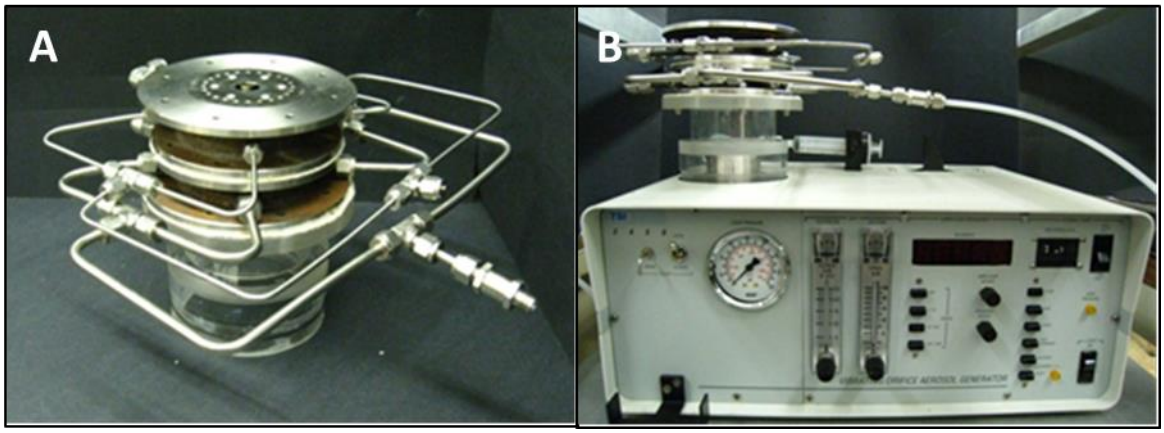

Figure 5. Photograph of the (**A**) burner assembly and (**B**) aerosol generator.

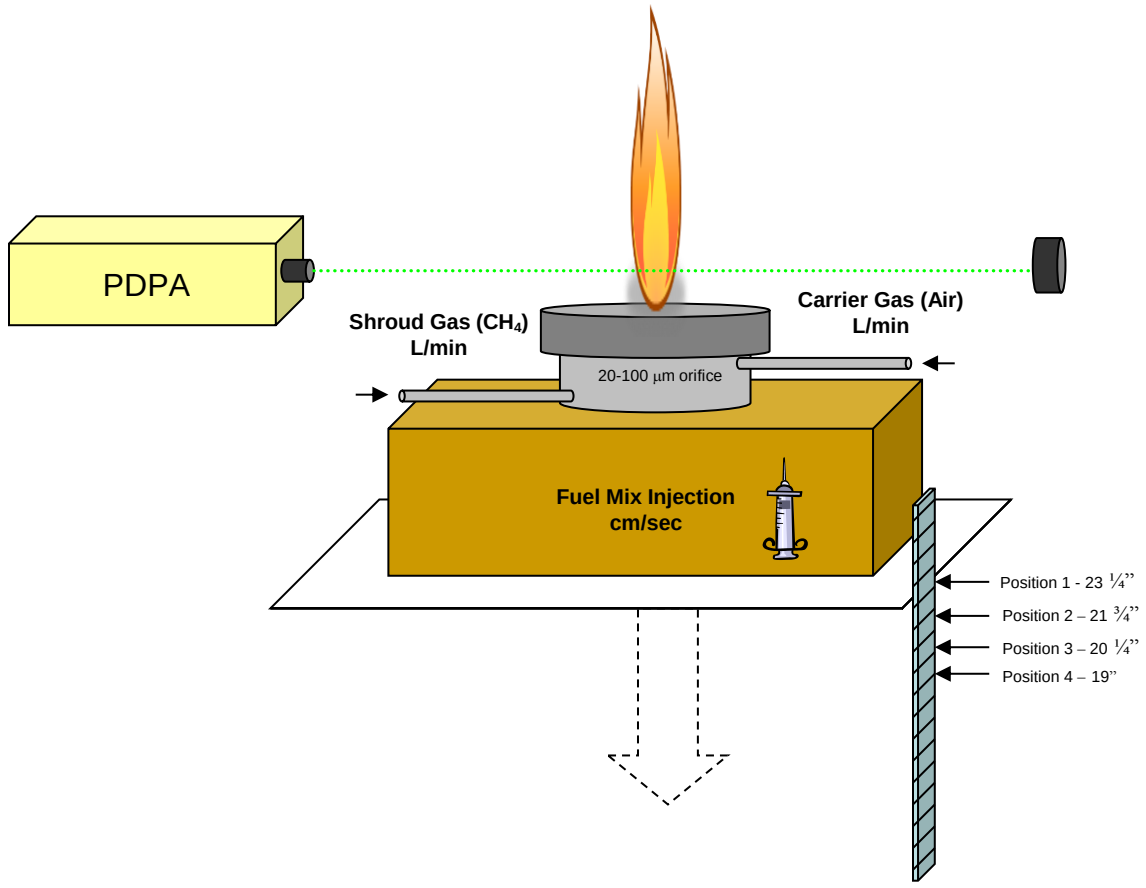

Figure 6. Diagram of benchtop flat flame burner unit showing injector nozzle assembly with VOAG orifice, fuel and gas supply showing optimal control flame rates, adjustable stage, and Aerometrics Phase-Doppler-Particle Analyzer (PDPA). Position 1, 2, 3, and 4 were fixed stage heights used during initial phase of this study.

Figure 7. Control flame using JP-at 2.5 x 10^{-3} cm/sec (JP-5 syringe injection speed); 8.5 L/min carrier gas (air) flow rate; 1.0 L/min shroud gas (methane) flow rate (shown with 20 μm injection orifice).

Table 1. Fuel mixtures tested.

Mixture	Base Fuel	Nanoparticle loading	Approximate Nanoparticle Mass Loading (%)
Control	JP-5	None	0
Mix-1	JP-5	~ 6 g Boron (coated w/ Oleic Acid) in ~ 300 ml JP-5	2.4
Mix-2	JP-5	~ 6 g Boron, 0.3 g Reduced CeO_2 (coated w/ Oleic Acid) in ~ 300 ml JP-5	2.5
Mix-3	JP-5	~ 6 g Boron, 0.3 g CeO_2 (coated w/ Oleic Acid) in ~ 300 ml JP-5	2.5
Mix-4	JP-5	~ 6 g CeO_2 (coated w/ Oleic Acid) in ~ 300 ml JP-5	2.4

Table 2. Summary of droplet size and velocity data for the JP-5 only F and W runs.

Fuel Mix	**JP-5**	**JP-5**	**JP-5**	**JP-5**	**JP-5**	**JP-5**	**JP-5**	**JP-5**
Wet (W) or Flame (F)	**F**	**F**	**F**	**F**	**W**	**W**	**W**	**W**
Ref Height (")	**23 1/4**	**21 3/4**	**20 1/4**	**19**	**23 1/4**	**21 3/4**	**20 1/4**	**19**
Total Dia. Counts	1091	1342	1530	1547	807	1385	1010	1249
Average Dia.(μm)	74.52	68.96	60.66	57.18	81.53	84.33	81.62	88.92
Std. Dev.	16.44	19.32	21.73	23.24	15.90	15.84	20.05	23.90
Min. Dia. (μm)	22.58	6.16	5.48	1.95	13.74	25.52	15.00	6.07
Max Dia. (μm)	151.15	146.44	125.72	161.17	143.78	139.36	163.74	156.46
Total Vel. Counts	1252	1496	1737	1803	944	1542	1304	1630
Average Vel. (m/sec)	3.10	3.53	3.55	2.60	2.63	2.33	1.39	1.03
Std. Dev.	0.71	0.67	0.72	1.12	0.98	0.80	0.57	0.50
Min. Vel. (m/sec)	0.64	0.30	0.23	0.20	0.30	0.05	0.05	0.05
Max. Vel. (m/sec)	4.82	4.99	5.69	5.08	5.11	4.54	3.65	3.32

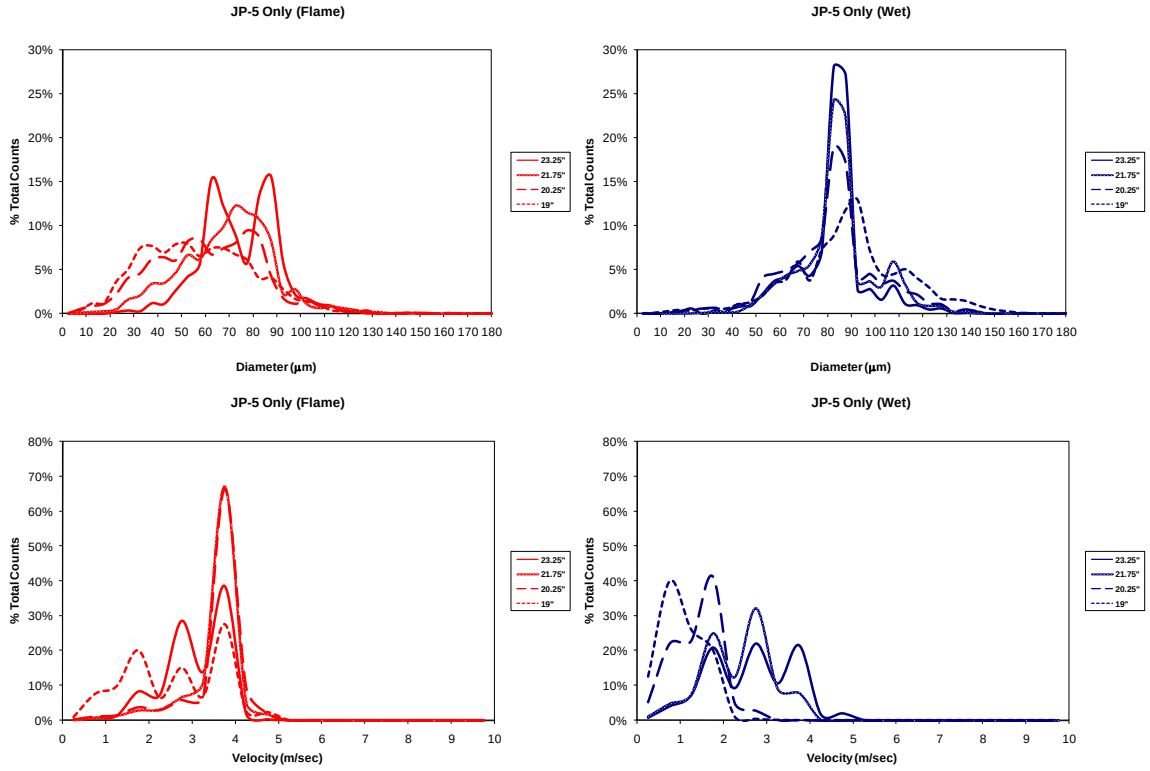

Figure 8. Droplet size and velocity plots at each stage height for JP-5 only F and W runs.

Table 3. Summary of droplet size and velocity data for Mix 1 F and W runs. Note: Mix 1 W run at the 23 ¼" stage height was not conducted.

Fuel Mix	**1**	**1**	**1**	**1**	**1**	**1**	**1**	**1**
Wet (W) or Flame (F)	**F**	**F**	**F**	**F**	**W**	**W**	**W**	**W**
Ref Height (")	**23 1/4**	**21 3/4**	**20 1/4**	**19**	**23 ¼**	**21 3/4**	**20 1/4**	**19**
Total Dia. Counts	433	383	390	468	-	155	319	322
Average Dia.(μm)	90.85	96.19	88.03	68.19	-	95.76	49.88	98.27
Std. Dev.	16.94	19.41	25.81	27.10	-	24.46	18.12	23.44
Min. Dia. (μm)	44.47	32.09	7.92	6.16	-	37.98	6.16	40.93
Max Dia. (μm)	137.01	154.53	158.23	149.15	-	166.77	123.57	170.60
Total Vel. Counts	489	425	438	552	-	176	402	440
Average Vel. (m/sec)	3.87	3.86	3.71	2.77	-	2.88	1.16	1.06
Std. Dev.	0.63	0.45	0.55	1.07	-	0.81	0.47	0.54
Min. Vel. (m/sec)	1.31	0.30	0.30	0.05	-	0.80	0.05	0.05
Max. Vel. (m/sec)	5.33	4.82	4.82	4.82	-	4.57	2.56	2.81

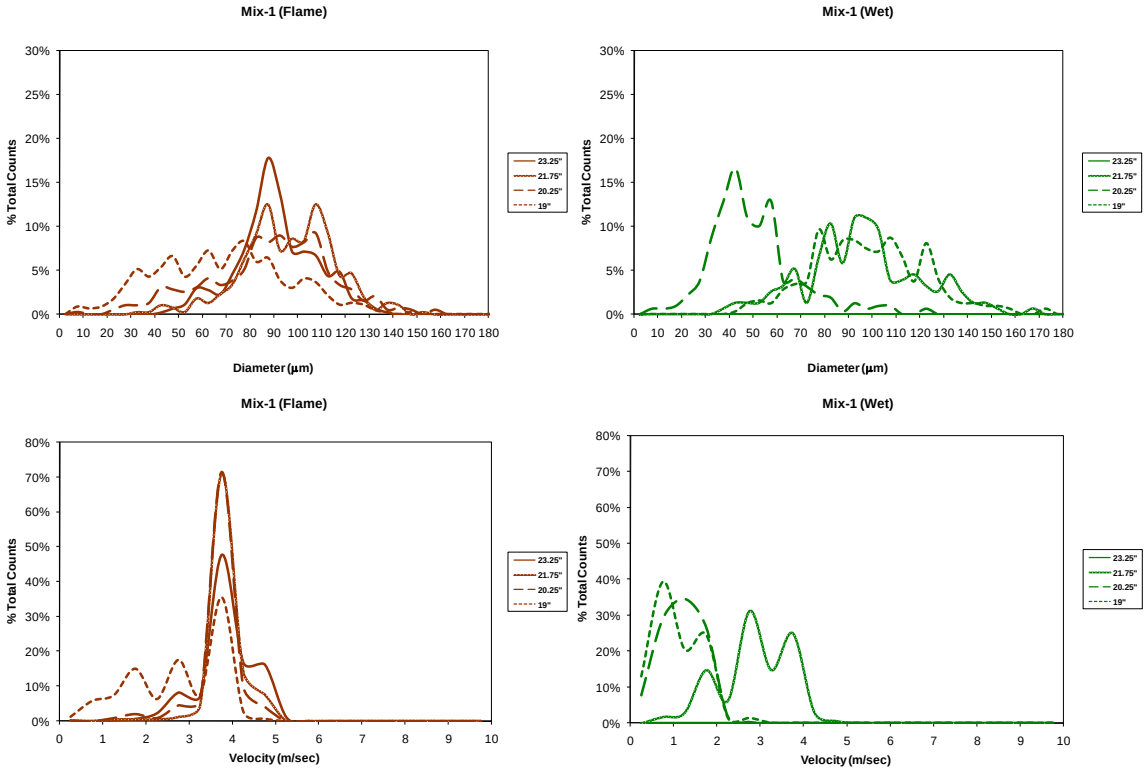

Figure 9. Droplet size and velocity plots at each stage height for the Mix 1 F and W runs. Note: Mix 1 W run at the 23 ¼" stage height was not conducted.

Table 4. Summary of droplet size and velocity data for Mix 2 F runs. Note: Mix 2 W runs were not conducted.

Fuel Mix	2	2	2	2	2	2	2	2
Wet (W) or Flame (F)	F	F	F	F	W	W	W	W
Ref Height (")	23 1/4	21 3/4	20 1/4	19	23 1/4	21 3/4	20 1/4	19
Total Dia. Counts	402	403	402	403	-	-	-	-
Average Dia.(μm)	76.04	78.02	75.32	70.59	-	-	-	-
Std. Dev.	21.45	21.27	22.50	25.03	-	-	-	-
Min. Dia. (μm)	8.81	16.47	17.06	4.68	-	-	-	-
Max Dia. (μm)	132.90	130.23	138.99	137.30	-	-	-	-
Total Vel. Counts	495	488	470	509	-	-	-	-
Average Vel. (m/sec)	3.05	3.79	3.36	3.04	-	-	-	-
Std. Dev.	0.78	0.52	1.00	1.00	-	-	-	-
Min. Vel. (m/sec)	0.30	1.31	0.05	0.30	-	-	-	-
Max. Vel. (m/sec)	4.82	5.33	4.82	5.33	-	-	-	-

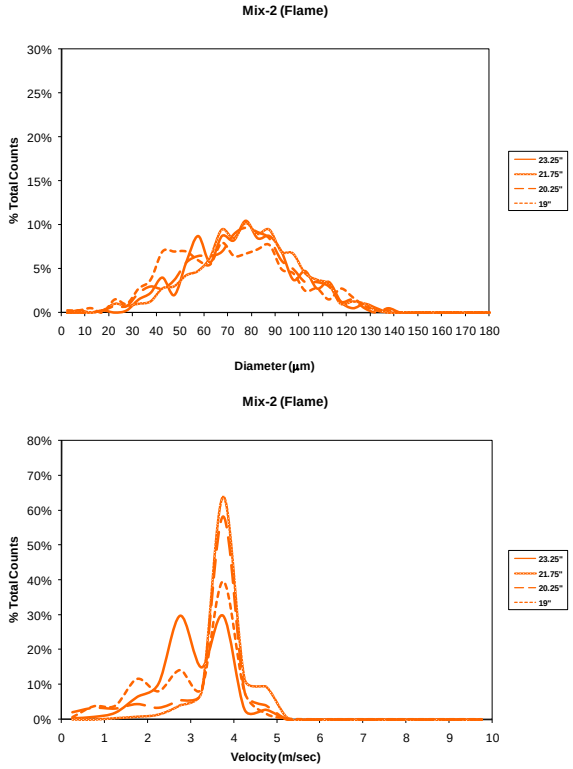

Figure 10. Droplet size and velocity plots at each stage height for Mix 2 F runs. Note: Mix 2 W runs were not conducted.

Table 5. Summary of droplet size and velocity data for Mix 3 F and W runs.

Fuel Mix	3	3	3	3	3	3	3	3
Wet (W) or Flame (F)	F	F	F	F	W	W	W	W
Ref Height (")	23 1/4	21 3/4	20 1/4	19	23 1/4	21 ¾	20 1/4	19
Total Dia. Counts	395	344	505	508	333	421	398	369
Average Dia.(μm)	99.02	84.21	77.87	67.35	80.97	77.60	77.26	79.67
Std. Dev.	20.62	21.36	23.18	24.31	17.48	21.46	22.53	23.77
Min. Dia. (μm)	14.11	13.38	2.03	6.75	18.53	10.87	12.05	6.75
Max Dia. (μm)	162.35	141.33	142.59	145.97	142.90	138.93	147.03	170.01
Total Vel. Counts	469	407	598	648	404	539	535	523
Average Vel. (m/sec)	3.63	3.65	3.53	2.72	3.16	2.36	1.26	0.90
Std. Dev.	0.72	0.51	0.68	1.03	0.95	0.81	0.54	0.44
Min. Vel. (m/sec)	0.80	0.30	0.30	0.23	0.80	0.30	0.05	0.05
Max. Vel. (m/sec)	6.84	4.82	4.82	4.82	5.33	4.82	2.81	2.31

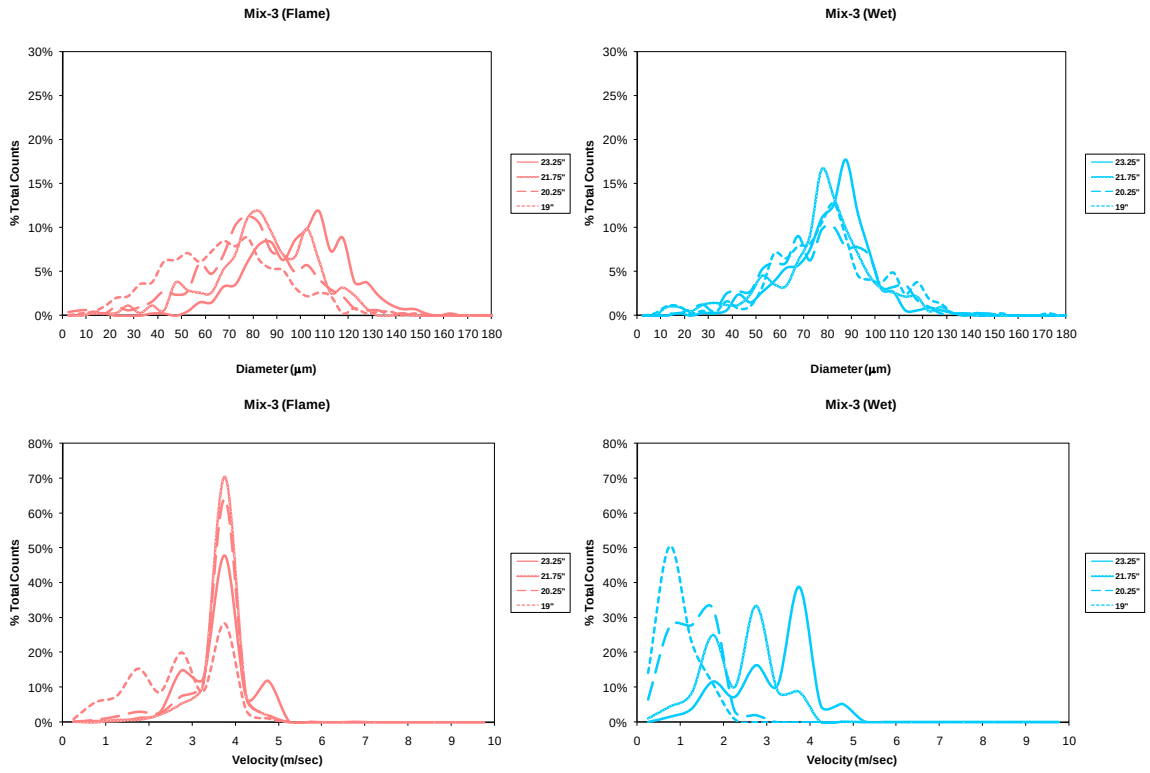

Figure 11. Droplet size and velocity plots at each stage height for Mix 3 F and W runs.

Table 6. Summary of droplet size and velocity data for Mix 4 F and W runs.

Fuel Mix	**4**	**4**	**4**	**4**	**4**	**4**	**4**	**4**
Wet (W) or Flame (F)	**F**	**F**	**F**	**F**	**W**	**W**	**W**	**W**
Ref Height (")	**23 1/4**	**21 3/4**	**20 1/4**	**19**	**23 1/4**	**21 3/4**	**20 1/4**	**19**
Total Dia. Counts	482	734	632	723	283	808	573	427
Average Dia.(μm)	74.81	74.02	75.82	74.38	77.74	83.29	84.36	85.24
Std. Dev.	18.95	30.35	65.37	48.94	19.72	19.01	18.12	25.18
Min. Dia. (μm)	13.15	10.79	2.54	2.93	7.25	6.66	13.74	3.80
Max Dia. (μm)	127.49	528.38	557.26	524.84	139.28	149.15	149.30	316.10
Total Vel. Counts	542	883	995	963	336	962	739	540
Average Vel. (m/sec)	3.15	3.82	3.57	3.78	2.76	2.63	1.57	0.94
Std. Dev.	0.77	0.49	0.78	2.08	0.91	0.75	0.62	0.45
Min. Vel. (m/sec)	0.80	0.30	0.30	0.30	0.64	0.30	0.05	0.05
Max. Vel. (m/sec)	4.82	5.33	5.83	11.11	5.08	4.57	3.82	2.31

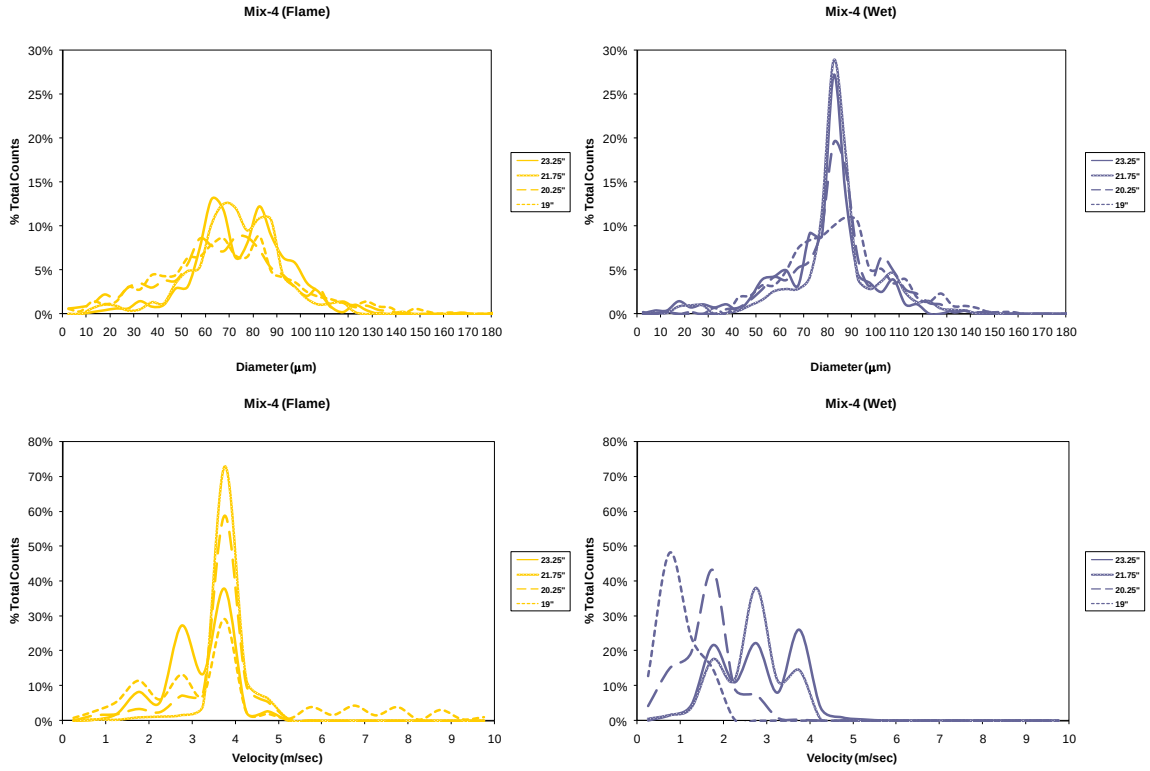

Figure 12. Droplet size and velocity plots at each stage height for Mix 4 F and W runs.

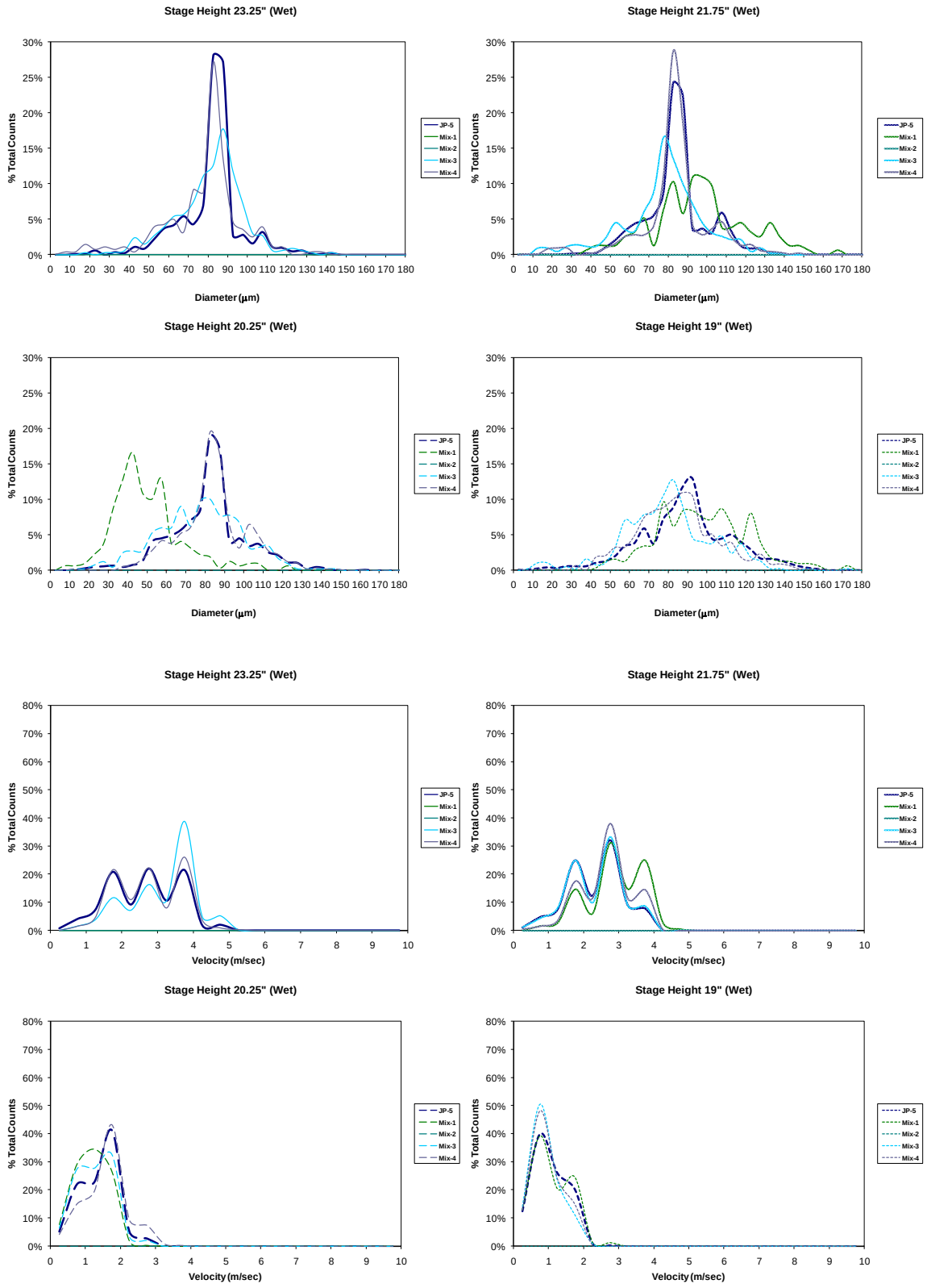

Figure 13. Droplet size and velocity plots for W runs at each stage height.

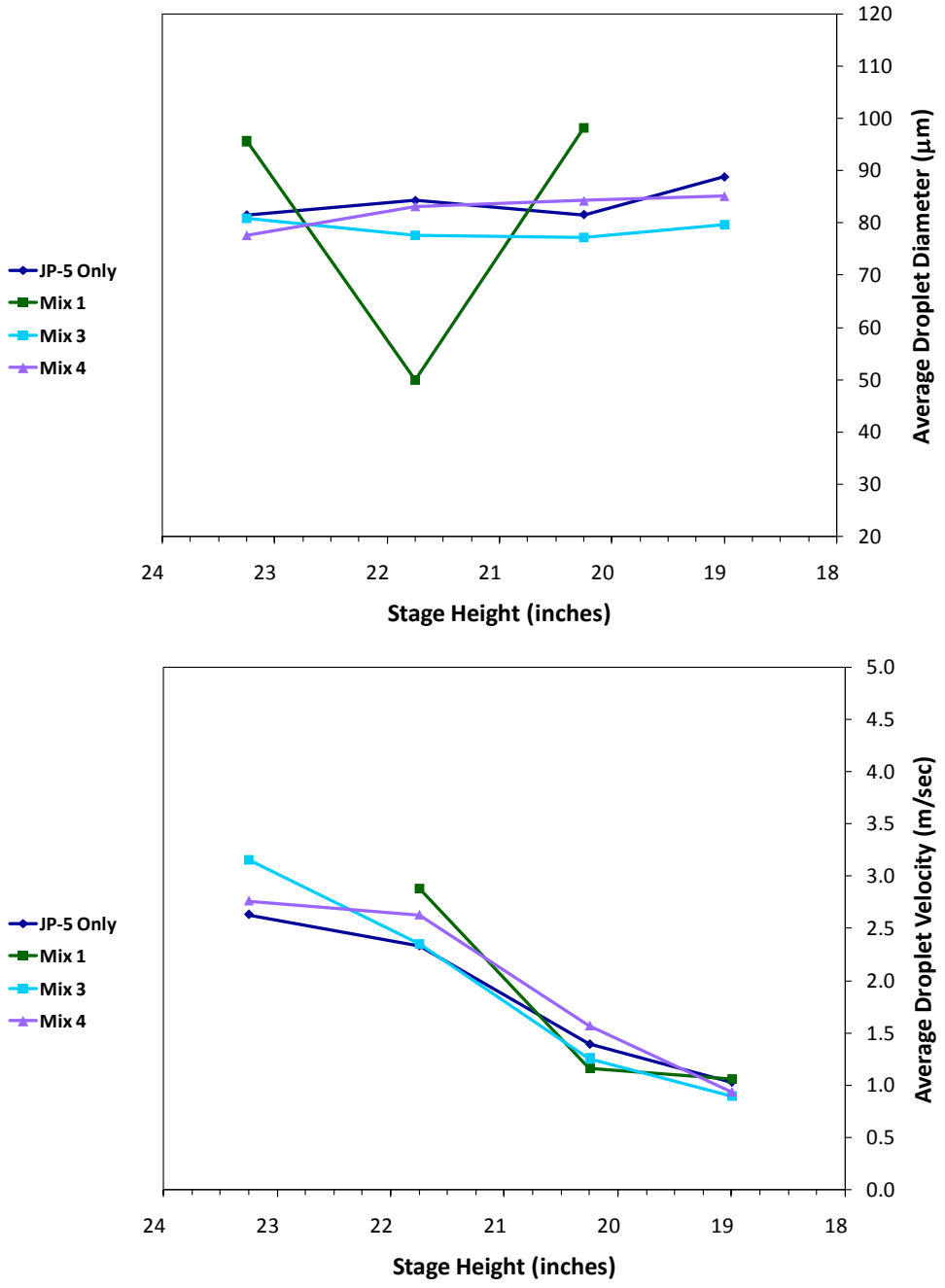

Figure 14. Average droplet size and velocity trends for W runs over measured stage heights.

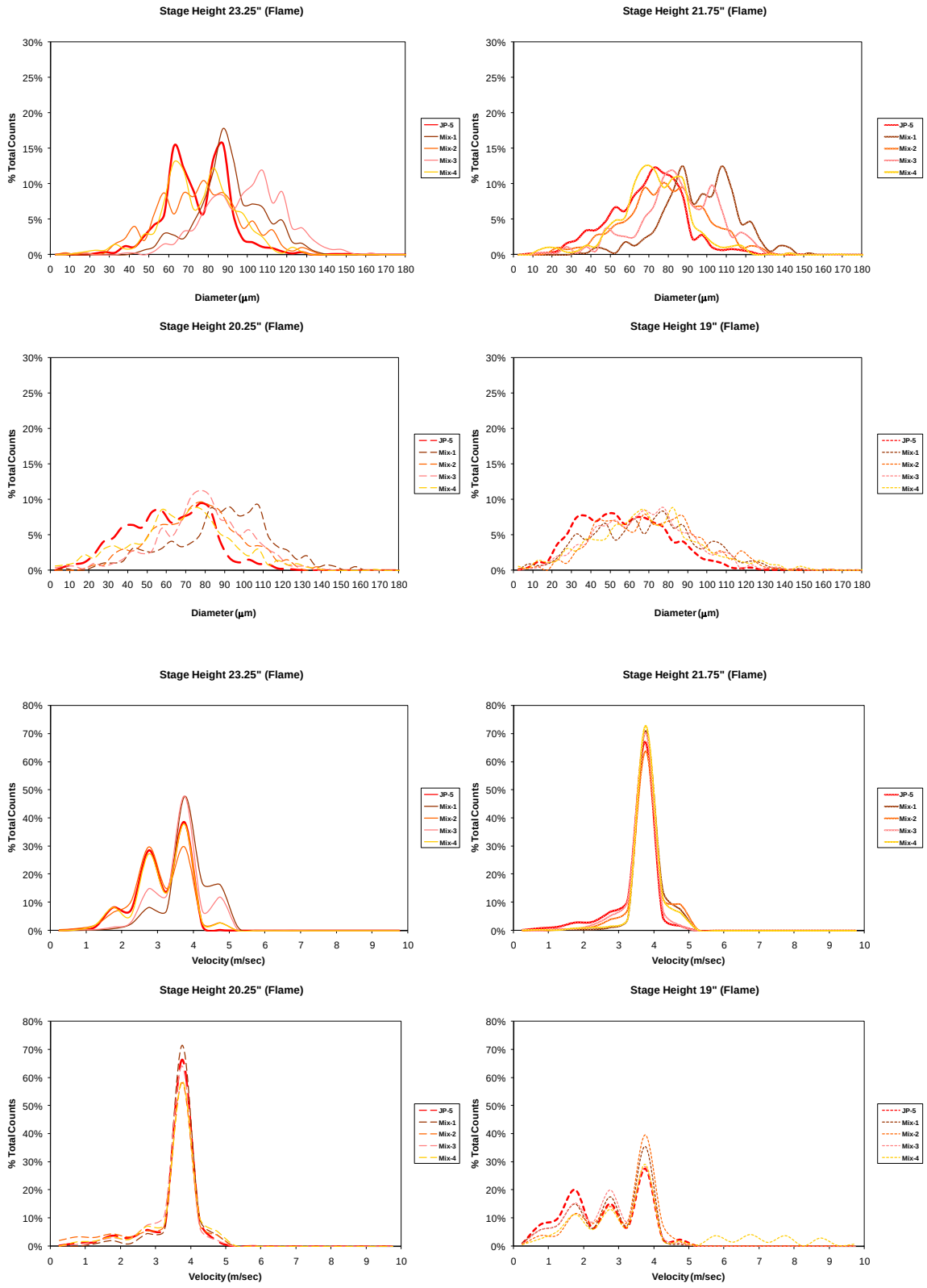

Figure 15. Droplet size and velocity plots for F runs at each stage height.

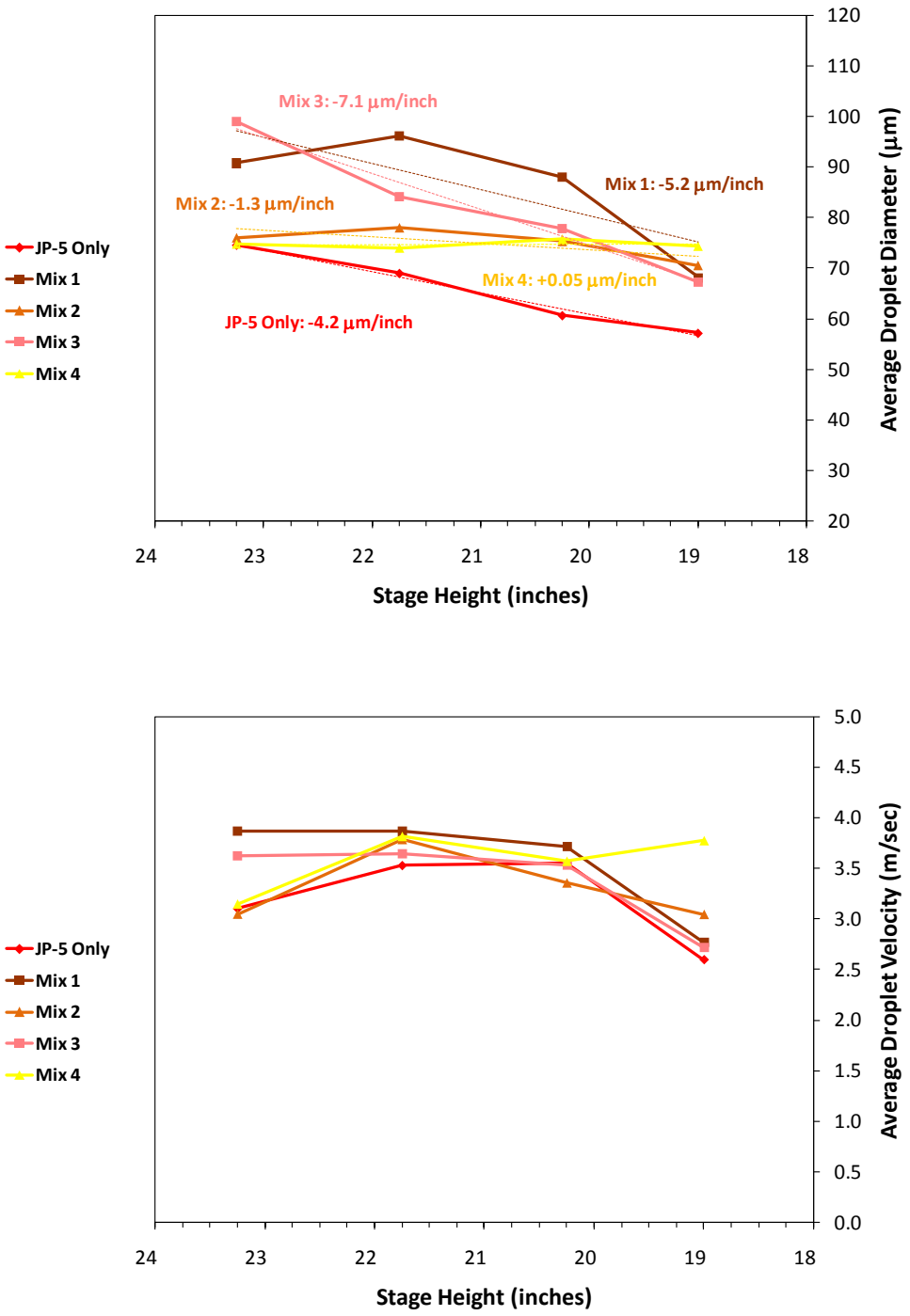

Figure 16. Average droplet size and velocity trends for F runs over stage heights.

Figure 17. Photograph of a $H_2/O_2/Ar$ + EtOH + boron-nanoparticle flame.

Figure 18. Close-up photograph of graduated cylinder containing boron-nanoparticle, JP-5 fuel slurry at ~2.5% loading during settling experiment.

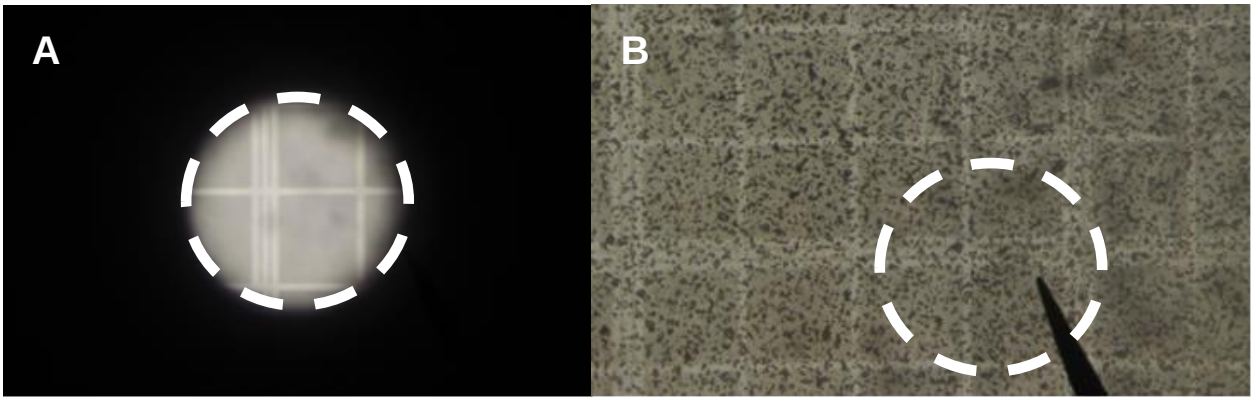

Figure 19. (**A**) Microscope photograph looking through the 100 μm VOAG orifice that clogged against a counting plate grid spacing of 50 μm. (**B**) Microscope photograph of a 1% w/v CeO_2 (w/ oleic acid) + JP-5 slurry against a counting plate grid spacing of 50 μm. Note: White-dashed circle indicates approximate diameter of 100 μm VOAG orifice.

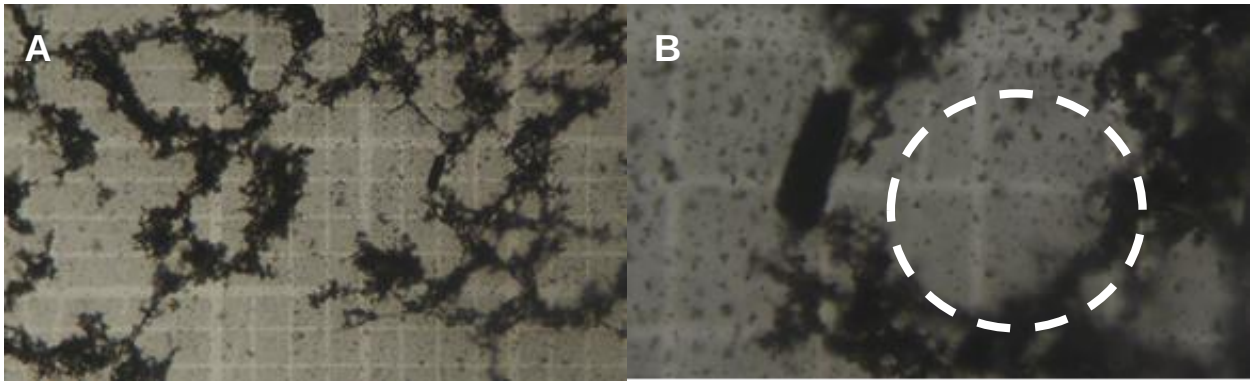

Figure 20. (**A**) Microscope photograph of a 1% w/v boron (w/ oleic acid) + JP-5 slurry against a counting plate grid spacing of 50 μm. (**B**) Microscope photograph showing same 1% w/v boron (w/ oleic acid) + JP-5 slurry under higher magnification. Note: White-dashed circle indicates approximate diameter of 100 μm VOAG orifice.

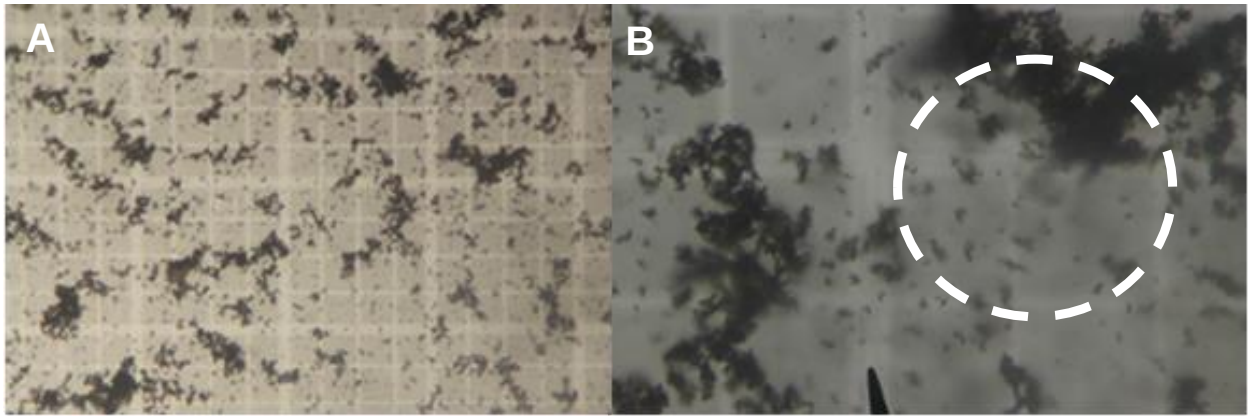

Figure 21. (**A**) Microscope photograph of a 0.1% w/v boron (w/ oleic acid) + JP-5 slurry against a counting plate grid spacing of 50 μm. (**B**) Microscope photograph showing same 0.1% w/v boron (w/ oleic acid) + JP-5 slurry under higher magnification. Note: White-dashed circle indicates approximate diameter of 100 μm VOAG orifice.